Microearthquake streaks and seismicity triggered by slow earthquakes on the mobile south flank of Kilauea Volcano, Hawai'i

Cecily J. Wolfe[1], Benjamin A. Brooks[1], James H. Foster[1], and Paul G. Okubo[2]

Submitted to *Geophysical Research Letters*, 2007

[1]School of Ocean and Earth Science and Technology, University of Hawai'i, 1680 East–West Rd, Honolulu, HI 96822, USA

[2]Hawaiian Volcano Observatory, US Geological Survey, Hawaii National Park, HI 96718, USA

Abstract: We perform waveform cross correlation and high precision relocation of both background seismicity and seismicity triggered by periodic slow earthquakes at Kilauea Volcano's mobile south flank. We demonstrate that the triggered seismicity dominantly occurs on several preexisting fault zones at the Hilina Pali. Regardless of the velocity model employed, the relocated earthquake epicenters and triggered seismicity localize onto distinct fault zones that form streaks aligned with the slow earthquake surface displacements determined from GPS. Due to the unknown effects of velocity heterogeneity and nonideal station coverage, our relocation analyses cannot distinguish whether some of these fault zones occur within the volcanic crust at shallow depths or whether all occur on the decollement between the volcano and preexisting oceanic crust at depths of ~8 km. Nonetheless, these Hilina Pali fault zones consistently respond to stress perturbations from nearby slow earthquakes.

1. Introduction

Slow (or 'silent') earthquakes (SEs) have now been found to occur repeatedly, and in some cases, periodically, in various tectonic settings such as subduction zones, strike-slip faults, and volcano flanks. Elucidating the fault processes and mechanical conditions that yield repeating or periodic slow slip events and associated phenomena such as tremor and triggered microseismicity are the subject of intensive ongoing research and monitoring. The observations and search for theoretical explanations have stimulated provocative hypotheses: for example, *Lowry* [2006] has proposed that periodicity of subduction zone SEs could arise as a resonant response to climate-driven stress perturbations.

In the past decade, Kilauea volcano's mobile south flank has been the site of 7 slow earthquakes identified from a continuous GPS (CGPS) network [*Cervelli et al*., 2002; *Brooks et al*., 2006; *Segall et al*., 2006]. *Brooks et al*. (2006) found that one spatially distinct family of 4 SEs is periodic and separated by 774+/-7 day periods during 1998-2005, although a subsequent 5th periodic SE failed to occur in the predicted time window in March 2007. Swarms of micoearthquakes are triggered by these SEs [*Brooks et al.,* 2006; *Segall et al*., 2006], with most occurring in a small localized region beneath the Hilina Pali (Figure 1). It is not yet known whether nonvolcanic tremor may also occur.

The periodic SEs accrue maximum surface displacements of a few cms over several hours to 2 days and have equivalent magnitudes of ~5.6-5.8 [*Brooks et al*., 2006]. These are small, but not insignificant, compared to the ~6-10 cm/yr regional average motions from relatively stable seaward sliding on a decollement extending from a depth of ~10 km below Kilauea volcano to where it approaches the seafloor offshore [e.g., *Owen*, 2000; *Morgan et al.*, 2000]. A first order question then is: do the SEs occur on the basal decollement in the offshore (updip) region and reflect a transitional region between stick-slip sliding onshore and stable sliding offshore? *Cervelli et al.* [2002] preferred a shallow (~5-6km deep) landward-dipping thrust fault located above the decollement as the source for the Nov. 2000 SE while *Brooks et al.* [2006] showed that the geodetic data permit many possible SE fault plane solutions ranging from shallow thrust faults, to deeper seaward-dipping normal faults, to subhorizontal decollement planes, although solutions generally place a substantial portion of the fault surface offshore. *Segall et al*. [2006] used relocations of triggered high-frequency earthquakes of the January 2005 SE, seismicity rate theory, and Coulomb stress modeling to suggest that it occurred offshore on the decollement at ~7-8 km depth.

Because the estimated depth of slow slip is difficult to constrain from the geodetic data alone [*Brooks and Frazer*, 2005; *Brooks et al*., 2006], the reliability of the Coulomb stress modeling for helping to constrain SE depth critically depends on the accuracy of estimated locations and mechanisms of the triggered seismicity. In their relocations, *Segall et al.* [2006] did not use the full waveform data; rather, they used a double-difference-derived mapping with manual HVO picks, assuming a 1D velocity model, between triggered events and previous high-precision relocations and tomography from elsewhere at Kilauea (*Hansen et al.* [2004]). *Segall et al.* [2006] also assumed a thrust mechanism with the basal decollement. In contrast, prior high precision relocation work by *Got and Okubo* [2003] using a combination of waveform correlation and handpicked travel time differences interpreted seismicity in this same region (including the events triggered by the Sep. 1998 SE) as occurring below the decollement on a steeply seaward-dipping plane and with a reverse mechanism. These two different interpretations of the seismicity patterns need to be resolved if the triggered events can be used reliably to help constrain SE location and mechanism. Here we perform double difference relocations [*Waldhauser and Ellsworth*, 2000] using high precision travel time differences from waveform cross correlation in order to help address this issue and to better illuminate the fine-scale characteristics of SE-triggered seismicity at the Hilina Pali.

2. Waveform cross correlation and relocation methodology

We obtained waveform data from the USGS Hawaiian Volcano Observatory (HVO) in the Hilina Pali region of SE-triggered seismicity (Figure 1) for 1203 earthquakes spanning the entire years of 2004 and 2005, as well as for periods of +/- 1 month around the dates of all identified Kilauea SEs [*Brooks et al*., 2006]. The cross correlation methodology for measured travel time differences generally followed the procedure in *Wolfe et al*. [2004] and double difference relocations used the method of *Waldhauser and Ellsworth* [2000]. *P* and *S* waves were sliced in windows of +/- 1.5 s around the predicted arrival time on vertical component seismometers. For cases where the predicted *S* minus *P* wave arrival time was less than 1.5 s and the *P* and *S* windows would overlap, only the *P*-wave data were correlated (alternatively excluding these cases was found to have little effect on the results). To reduce outliers from noisy stations, the correlations used only the best 30 stations in the HVO seismic network, as indicated by handpicked travel times (Figure 1a).

Tests demonstrate that the assumed 1-D velocity model has a significant influence on the absolute depths of the relocations (auxiliary Text S1 and auxiliary Figures S1 and

S2). Our preferred velocity model contains slower-than-typical mid-crustal velocities (auxiliary Figure S3), as has been observed at the Hilina Pali [*Hansen et al.*, 2004; Park et al., 2007], but as discussed below the effects of unknown velocity heterogeneity may have important influence.

3. Results

Figures 2 and 3 display the results of high precision relocation of 891 earthquakes, along with the patterns of relocated triggered seismicity on the days of 3 slow earthquakes on 1/26/2005, 9/19/1998, and 11/9/2000 (the slow earthquake of 12/16/2002, with smallest magnitude, produced few triggered earthquakes). The triggered seismicity consistently relocates on several distinct clusters, or fault zones, with depths varying from 5 km to 7 km (see auxiliary material demonstrating how the absolute depths can vary with differing 1-D velocity models). While the epicenters for the original HVO locations are diffuse clouds (Figure 2), after relocation, epicenters collapse into several distinct clusters that form streaks aligned nearly parallel to the geodetically defined slip direction of SEs from GPS data [*Brooks et al*., 2005]. After relocation, the depths of earthquakes also collapse from diffuse cloud at 4-9 km depth to several compact clusters that are each more localized in depth (Figure 3). The absolute depth of each cluster can vary with assumed velocity model.

The most active fault zone, and on which triggered seismicity also dominantly occurs, was studied by *Got and Okubo* [2003], who imaged a strongly southeast dipping fault zone and suggested that this fault is not the decollement but rather a deeper reverse fault with conjugate sense faulting. Our relocations do not image such a dipping fault

(Figure 3), but rather result in a horizontally aligned band of earthquakes that tends to be shallow (4-6 km depth). A composite focal mechanism for earthquakes on this fault zone using first motion polarities displays one fault plane with seaward slip on a low-angle plane (Figure 2). These observations suggest that this fault plane may be near horizontal with seaward slip, and not strongly dipping.

However, we are concerned that poor station geometry as well as velocity heterogeneity may be biasing the absolute depth of our relocations and our analyses may not be capable of distinguishing between a fault zone located at shallow depths within the volcanic crust or a fault zone located at the decollement interface between the volcano and preexisting oceanic crust (near 8 km depth). Because this region is near the coast, the azimuthal distribution of stations is suboptimal (Figure 1) and there are no stations to the south of this region. In addition, nearby station coverage to the east is poor, because station KAE (Figure 1b) was noisy and provided few travel time differences (stations HLP and AHU yielded ~10,000 travel time difference measurements, POL yielded ~6,000, whereas KAE yielded only ~800).

Strong (as much as ~15%) velocity heterogeneity observed at the Hilina Pali can vary over horizontal distances on the order of 5 km [*Hansen et al.,* 2001], which means that the entire ray paths from the source region to stations outside the Hilina Pali are likely not well approximated by any 1-D velocity model. Because the fault zone of interest spans several kilometers distance, double difference relocations have some sensitivity to absolute location [*Wolfe*, 2002; *Menke and Schaff*, 2004], but coupling this sensitivity with a velocity model that does not correctly account for strong heterogeneity may possibly lead to erroneous absolute depths. We have recently deployed a temporary network of 11 additional station sites in this region and expect that future work involving double difference tomography [*Zhang and Thurber*, 2003] will be able to resolve these issues.

4. Discussion and Conclusions

Although our high precision relocations of triggered seismicity at the Hilina Pali cannot constrain the absolute depths and whether triggered seismicity occurs on the decollement or within the volcano, earthquake patterns nonetheless collapse into several streaks of seismicity that are aligned parallel to the GPS vectors of SE slip (Figure 2) and have narrow depth extent (Figure 3). Interestingly, the orientations of streaks are more closely aligned with the GPS measured surface displacement directions of intermittent SEs than with the surface displacement directions inferred to result from long-term decollement creep (Figure 2).

Inspection of less accurate catalog locations suggests that these Hilina seismicity streaks are features that have persisted for at least 40 years, since the beginning of high quality HVO monitoring for this region in the late 1960s. Similar types of concentrated streaks of microseismicity aligned in the slip direction have been observed in many regions [e.g., *Gillard et al*., 1996; *Rubin et al*., 1999]. Streaks are generally interpreted as reflecting heterogeneity in the frictional properties of the fault. One suggestion is that seismicity streaks are caused by regions of unstable (stick-slip/velocity weakening) sliding surrounded by larger regions of stable sliding (creep/velocity strengthening) [e.g., *Rubin et al*., 1999]; another suggestion is that seismicity streaks occur as alignments along a boundary between a locked and creeping section [e.g., *Sammis and Rice*, 2001].

The underlying cause of this type of structural organization of a fault surface and how it affects rupture dynamics remains a topic of much interest, with modeling studies indicating that the interaction between velocity strengthening and velocity weakening regions is also important in the occurrence of slow earthquakes [*Kato*, 2004; *Liu and Rice*, 2005]. Eventual constraint on the depth of Hilina Pali streaks will be key to further understanding their tectonic and frictional implications. For example, if it is later demonstrated that these microearthquakes do occur on the decollement, then why is there a seaward protruding band of earthquakes here, unlike the decollement seismicity to the east that occurs in a narrow onshore strip parallel to the east rift zone (Figure 1)? One possibility is that the Hilina protrusion of seismicity might be associated with a more complex stress field (and stress history) created by the intersection of the east rift and south west rift zones. Another possibility is that the seismicity may be related to a physical anomaly on the seafloor interacting with the overriding plate, such as a seamount, as it underthrusts the Hilina slump.

Regardless of the tectonic characterization of the Hilina streaks, Figure 2 demonstrates that they respond to the stress perturbations produced by the nearby slow earthquakes. This behavior is consistent with the previous results of *Dieterich et al*. [2000], who compared rate and state friction stress predictions and independent estimates to demonstrate that Kilauea's decollement seismicity east of our study region is a reliable stress meter of nearby diking events and moderate earthquakes.

Acknowledgments: This research was funded by the Geophysics and Petrology and Geochemistry Programs of the US National Science Foundation and the USGS.

References:

Brooks, B.A., and L. N. Frazer (2005), Importance reweighting reduces dependence on temperature in Gibbs samplers; an application to the coseismic geodetic inverse problem , *Geophys. J. Int., 161*, 12-20.

Brooks, B.A., Foster, J.H., Bevis, M.F., L.N., Wolfe, C.J., and Behn, M. (2006), Periodic slow earthquakes on the flank of Kilauea volcano, Hawai'i, *Earth Planet. Sci. Lett., 246*, 207-216.

Cervelli, P., Segall, P., Johnson, K., Lisowski, M., and Miklius, A. (2002), Sudden aseismic fault slip on the south flank of Kilauea volcano, *Nature, 415*, 1014-1018.

Dieterich, J., V. Cayol, and P. Okubo (2000), The use of earthquake rate changes as a stress meter at Kilauea volcano, *Nature, 408*, 457-460.

Gillard, D., A. M. Rubin, and P. Okjubo (1996), Highly concentrated seismicity caused by deformation of Kilauea's deep magma system, *Nature, 384*, 343-346.

Got, J.-L., and P. Okubo (2003), New insights into Kilauea's volcano dynamics brought by large-scale relative relocation of microearthquakes, *J. Geophys. Res., 108*, doi:10.1029/2002JB002060.

Hansen, S., C. Thurber, MJ. Mandernach, F. Haslinger, and C. Doran (2004), Seismic velocity and attenuation structure of the east rift zone and south flank of Kilauea volcano, Hawaii, *Bull. Seismol. Soc. Am., 94*, 1430-1440.

Kato, N. (2004), Interaction of slip on asperities: Numerical simulation of seismic cycles on a two-dimensional planar fault with nonuniform frictional property: *Journal of Geophysical Research*, v. 109, p. doi:10.1029/2004JB003001.

Liu, Y., and J. R. Rice (2005), Aseismic slip transients emerge spontaneously in 3d rate and state modeling of subduction earthquake sequences, J. Geophys. Res., 105, 18,983-18,998.

Lowry, A. R. (2006), Resonant slow fault slip in subduction zones forced by climatic load stress, *Nature, 442*, 802-805, 2006.

Menke, W. and D. Schaff (2004), Absolute locations with differential data, *Bull. Seismol. Soc. Am., 94*, 2254-2264.

Morgan, J.K., G.F. Moore, D.J. Hills, and S. Leslie (2000), Overthrusting and sediment accretion along Kilauea's mobile south flank, Hawaii: Evidence for volcanic spreading from marine seismic reflection data, *Geology, 28*, 667-670.

Owen, S., Denlinger, R., Sako, M., Segall, P., Lisowski, M., and Miklius, A. (2000), Rapid deformation of Kilauea Volcano: Global Positioning System measurements between 1990 and 1996: *Journal of Geophysical Research B: Solid Earth*, v. 105, p. 18,983-18,998.

Park, J., J. K. Morgan, C. A. Zelt, P. G. Okubo, L. Peters, and N. Benesh (2007), Comparitive velocity structure of active Hawaiian volcanoes from 3-D onshore-offshore seismic tomography, *Earth Planet. Sci. Lett., 259*, 500-516.

Rubin, A. M., D. Gillard, and J.-L. Got (1999), Streaks of microearthquakes along creeping faults, *Nature, 400*, 635-641.

Sammis, C. G., and J. R. Rice (2001), Repeating earthquakes as low-stress drop events at a border between locked and creeping fault patches, *Bull. Seismolog. Soc. Am., 91*, 532-537.

Segall, P., Desmarais, E.K., Shelly, D., Miklius, A., and Cervelli, P. (2006), Earthquakes Triggered by Silent Slip Events on Kilauea Volcano, Hawaii, *Nature, 442*, 71-74; correction (2006), *Nature, 444*, 235.

Waldhauser, F., and W. L. Ellsworth, A double-difference earthquake location algorithm: Method and application to the Northern Hayward fault (2000), *Bull. Seismol. Soc. Am*. *90*, 1353-1368.

Wolfe, C. J. (2002), On the mathematics of using difference operators to relocate earthquakes, *Bull. Seismol. Soc. Am., 92*, 2879-2892.

Wolfe, C.J., P.G. Okubo, G. Ekström, M. Nettles, and P. Shearer, Characteristics of deep (> 13 km) Hawaiian earthquakes and Hawaiian earthquakes west of 155.55°W (2004), *Geochem. Geophys. Geosys., 5,* doi:10.1029/2003GC000618.

Zhang, H., and C. H. Thurber, Double-difference tomography: The method and its application to the Hayward fault, California (2003), *Bull. Seismol. Soc. Am., 93*, 1875-1889.

Figure captions:

Figure 1. a) Location of the subset of 30 seismometers used for waveform cross correlation. b) Triggered seismicity (red circles) from the USGS ANSS catalog on January 26, 2005, the time period of a slow earthquake at Kilauea. Note the large number of earthquakes in the boxed region chosen for this high precision relocation study, where typical background rates for this region are 1 earthquake per day. The names of nearby seismic stations are shown and background seismicity at 5-13 km depth for the years 2002-2007 is also plotted (gray circles).

Figure 2. High precision relocations using waveform cross correlation data. The seismicity for the total dataset is given as filled circles color-coded by depth. Earthquakes triggered by 3 slow earthquakes on a) 1/26/2005, b) 9/19/1998, and c) 11/9/2000 are given as black circles, and d) original HVO locations are also shown. The number of triggered earthquakes (N) for each date is also denoted. Composite focal mechanism is shown for the fault zone studied by *Got and Okubo* [2003]. Arrows indicate the GPS directions for decollement creep (gray arrows) and the slow earthquake of Jan. 2005 (red arrows).

Figure 3. Plot of depth versus latitude for the earthquakes shown in Figure 2 (color coded by longitude). a) Relocated earthquakes. b) Original HVO locations.

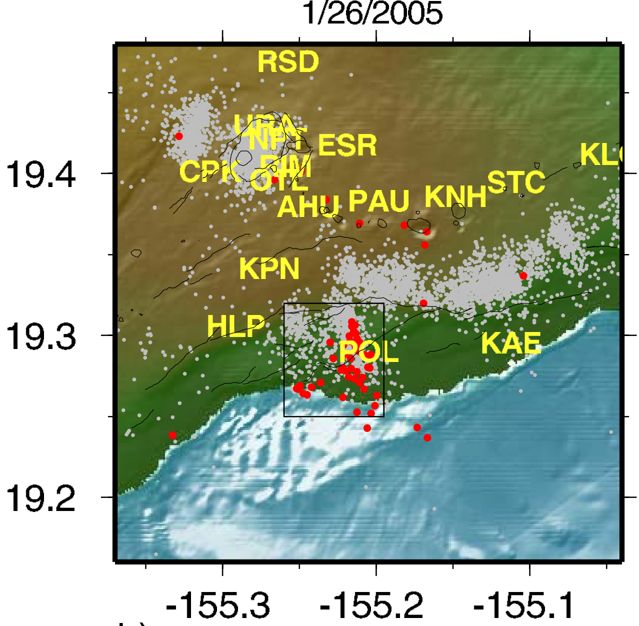
1/26/2005
RSD
ESR
CPK
AHU
PAU
KNH
STC
KPN
HLP
POL
KAE
19.4
19.3
19.2
-155.3
-155.2
-155.1

b)

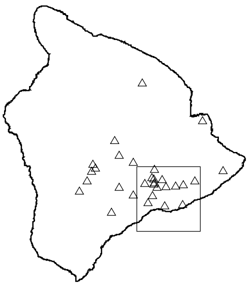

a)

Figure 1

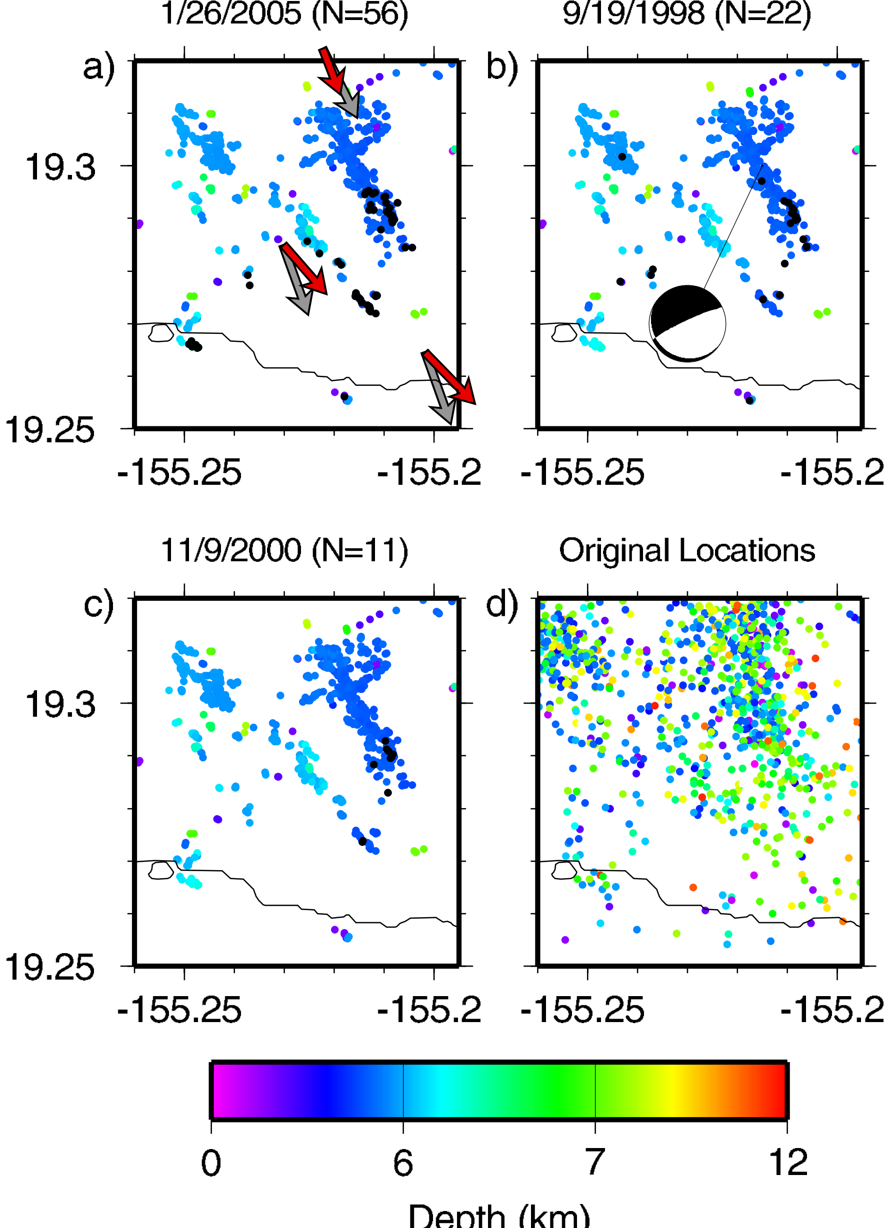

1/26/2005 (N=56)
9/19/1998 (N=22)
a)
b)
19.3
19.25
-155.25
-155.2
11/9/2000 (N=11)
Original Locations
c)
d)
0
6
7
12
Depth (km)

Figure 2

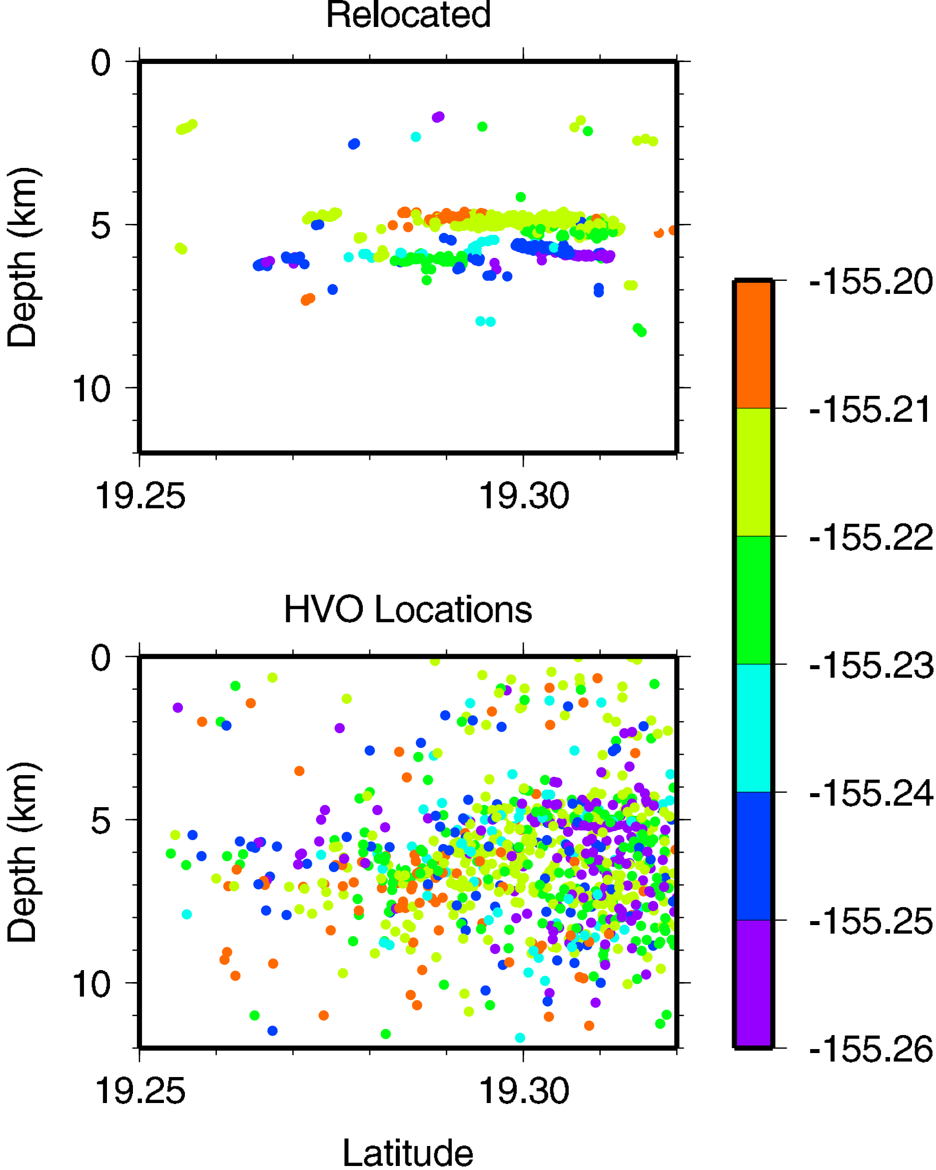

Relocated
0
5
10
Depth (km)
19.25
19.30
HVO Locations
0
5
10
Depth (km)
19.25
19.30
Latitude
-155.20
-155.21
-155.22
-155.23
-155.24
-155.25
-155.26

Figure 3